Comparison of Anti-Obesity Effects of Ginger Extract Alone and Mixed with Long Pepper Extract

Gunju Song , Hyein Han , Heegu Jin , Jongwon Kim , Boo-Yong Lee *

Posted Date: 30 June 2025

doi: 10.20944/preprints202506.2436.v1

Keywords: browning; lipid accumulation; thermogenesis; ginger extract; long pepper extract; metabolic syndrome

 doi:10.20944/preprints202506.2436.v1

Article

Comparison of Anti-Obesity Effects of Ginger Extract Alone and Mixed with Long Pepper Extract

Gunju Song, Hyein Han, Heegu Jin, Jongwon Kim and Boo-Yong Lee *

Department of Food Science and Biotechnology, College of Life Science, CHA University, Seongnam, Gyeonggi 13488, Republic of Korea

* Correspondence: bylee@cha.ac.kr; Tel.: +82-31-881-7155

Abstract

Obesity is a chronic metabolic disorder characterized by the excessive expansion of adipose tissue and impaired energy homeostasis. This study evaluated the anti-obesity effects of ginger (Zingiber officinale Roscoe) extract, as well as a mixture of ginger extract and long pepper (*Piper longum L.*) extract, in high-fat diet-induced obese mice. Mice were orally administered ginger extract (60 mg/kg/day) or a mixture of ginger extract and long pepper extract (1:1 ratio, 30 mg/kg/day each) for 8 weeks. Treatment with ginger extract alone significantly reduced body weight gain and visceral and subcutaneous fat mass compared to high-fat diet group. In contrast to the ginger extract alone, the mixture of long pepper extract resulted in less pronounced anti-obesity benefits. Ginger extract promotes lipolysis through the activation of the protein kinase A (PKA) signaling pathway and induces the browning of white adipose tissue by upregulating uncoupling protein 1 (UCP1) expression. Notably, ginger extract alone demonstrated superior anti-obesity effects by improving glucose homeostasis and lipid profiles, as well as modulating adipose tissue metabolic processes more effectively than the mixture of ginger extract and long pepper extract. These findings indicate that ginger extract may serve as a promising natural agent for the prevention and management of obesity-related metabolic dysfunction.

Keywords: browning; lipid accumulation; thermogenesis; ginger extract; long pepper extract; metabolic syndrome

1. Introduction

Obesity is a complex and chronic metabolic disorder characterized by the excessive accumulation of adipose tissue and the disruption of normal glucose homeostasis [1–3]. This abnormal fat accumulation not only indicates energy imbalance but also leads to various metabolic dysfunctions [4]. As fat mass increases, particularly in visceral fat, it induces a state of low-grade, chronic inflammation that interferes with insulin action, exacerbating insulin resistance and impairing glucose homeostasis [5]. Over time, this metabolic dysregulation significantly increases the risk of developing various conditions associated with metabolic syndrome, including hyperlipidemia, hypertension, impaired glucose tolerance, and non-alcoholic fatty liver disease (NAFLD) [6]. These comorbidities are major risk factors for cardiovascular disease and type 2 diabetes [7].

White adipose tissue (WAT), traditionally considered as merely an energy reservoir, is now recognized as a highly dynamic endocrine organ that secretes a variety of adipokines and inflammatory cytokines, which regulate lipid and glucose metabolism [5,8]. The expansion of WAT occurs through two primary mechanisms: hypertrophy, characterized by an increase in the size of adipocytes, and hyperplasia, defined as an increase in the number of adipocytes [9–11]. Hyperplasia is regulated at the transcriptional level by key adipogenic factors such as CCAAT/enhancer-binding protein alpha (C/EBPα), peroxisome proliferator-activated receptor gamma (PPARγ), and fatty acid-binding protein 4 (FABP4), which coordinate the differentiation of preadipocytes into fully

 doi:10.20944/preprints202506.2436.v1

differentiated adipocytes enriched in intracellular lipids [12–14]. During hypertrophy, mature adipocytes accumulate lipids, a process in which lipogenic enzymes such as lysophosphatidic acid acyltransferase theta (LPAATθ), lipin 1, and diacylglycerol acyltransferase 1 (DGAT1) play a critical role [15,16]. These enzymes catalyze the sequential reactions involved in triglyceride biosynthesis, facilitating lipid storage in adipose tissue [17].

Lipolysis is the catabolic breakdown of triglycerides into free fatty acids (FFAs) and glycerol, thereby supporting energy metabolism [18,19]. This process is primarily initiated by protein kinase A (PKA), which activates a lipase cascade involving adipose triglyceride lipase (ATGL), phosphorylated hormone-sensitive lipase (p-HSL), and monoacylglycerol lipase (MGL) [20]. The liberated FFAs can be oxidized within adipocytes or transported to peripheral tissues such as the liver, heart, and skeletal muscle for energy utilization [21]. In contrast to energy storage, brown adipose tissue (BAT) dissipates energy as heat via non-shivering thermogenesis mediated by uncoupling protein 1 (UCP1) [22,23]. Under specific stimuli, white adipocytes can undergo a phenotypic transition known as "browning," which is characterized by the upregulation of thermogenic genes including peroxisome proliferator-activated receptor alpha (PPARα), PPARγ coactivator 1-alpha (PGC1α), PR domain-containing 16 (PRDM16), and UCP1, offering a potential mechanism to increase energy expenditure and combat obesity [24,25].

Ginger (Zingiber officinale) extract (GE) has consistently demonstrated anti-obesity effects and is regarded as a promising candidate for managing diet-induced metabolic disorders [26–28]. Based on previous studies, GE was administered at 60 mg/kg/day to evaluate its metabolic efficacy. Long pepper (Piper longum L.) extract (LPE), which contains the bioactive compound piperine, has also shown potential to modulate lipid metabolism and enhance metabolic function [29,30]. In this study, LPE was co-administered with ginger extract at a 1:1 ratio to evaluate potential synergistic effects. The LPE dose (30 mg/kg/day) was determined based on the acceptable daily intake (ADI) of piperine for humans, as defined by the European Food Safety Authority (EFSA), and was converted to an equivalent dose for mice [31]. The dose used in this study was within the safe intake established by the revised no-observed-adverse-effect level (NOAEL). The aim of this study is to examine the anti-obesity effects of GE alone and in combination with LPE to compare their relative efficacy in a high-fat diet (HFD)-induced obesity model.

2. Materials and Methods

2.1. Preparation and Standardization of Ginger and Long Pepper Extracts

The GE was used as Ginginoll that was manufactured by AKAY Natural Ingredients Private Limited. (Kerala, India) and provided by Ju Yeong NS Co., Ltd. (Seoul, Korea). To confirm the synergistic effect with the GE, LPE used in the mixture (GE+LPE) was manufactured by Ju Yeong NS Co., Ltd. and is standardized to Piperine≤ 2%. For this experiment, it was administered after being mixed with the ginger extract in a 1:1 ratio based on weight for use.

GE was prepared from the dried rhizomes of Zingiber officinale Roscoe, and LPE was derived from the dried fruits of Piper longum L. GE was prepared via supercritical CO_2 extraction from dried ginger rhizomes followed by blending with arabic gum and maltodextrin, spray-drying, and standardizations. LPE was prepared by 65% ethanol extraction of dried long pepper fruits, followed by concentration, blending with arabic gum, spray-drying, and final standardization. The nutritional composition and marker compounds of both extracts were analyzed to assess functional characteristics (Table 1). Total polyphenol content (TPC) was measured using the Folin–Denis method, and the results were expressed as mg gallic acid equivalents (GAE) per gram of extract.

Table 1. Composition of Ginger Extract (GE) and Long Pepper Extract (LPE).

Component	Ginger extract (GE)	Long pepper extract (LPE)
Energy (kcal/100g)	623.49	357.85
Carbohydrate (%)	39.96	86.30

 doi:10.20944/preprints202506.2436.v1

Crude fat (%)	51.21	0.45
Crude protein (%)	0.69	2.15
Ash (%)	5.10	5.38
Moisture (%)	3.04	5.72
Total polyphenols (GAE mg/g)	139.4 ± 2.7	5.6 ± 0.1
Marker compound content (mg/g)	6-gingerol: 132	piperine: 20

Marker compounds were quantified by high-performance liquid chromatography (HPLC) equipped with a photodiode array detector (PDA). Analyses were performed using a Waters Arc HPLC series equipped with a C18 column (4.6 × 250 mm, 5 µm; Luna C18(2)). The mobile phase was acetonitrile and distilled water with 1% acetic acid (65:35, isocratic) at 1.0 mL/min. The detection wavelength was set at 280 nm, the column was maintained at 35 °C, and the injection volume was 10 µL. Under these conditions, the retention times were 5.036 min for 6-gingerol and 5.694 min for piperine. The concentrations of 6-gingerol in GE and piperine in LPE were 132 mg/g and 20 mg/g, respectively. A representative HPLC chromatogram of each extract is shown in Figure 1.

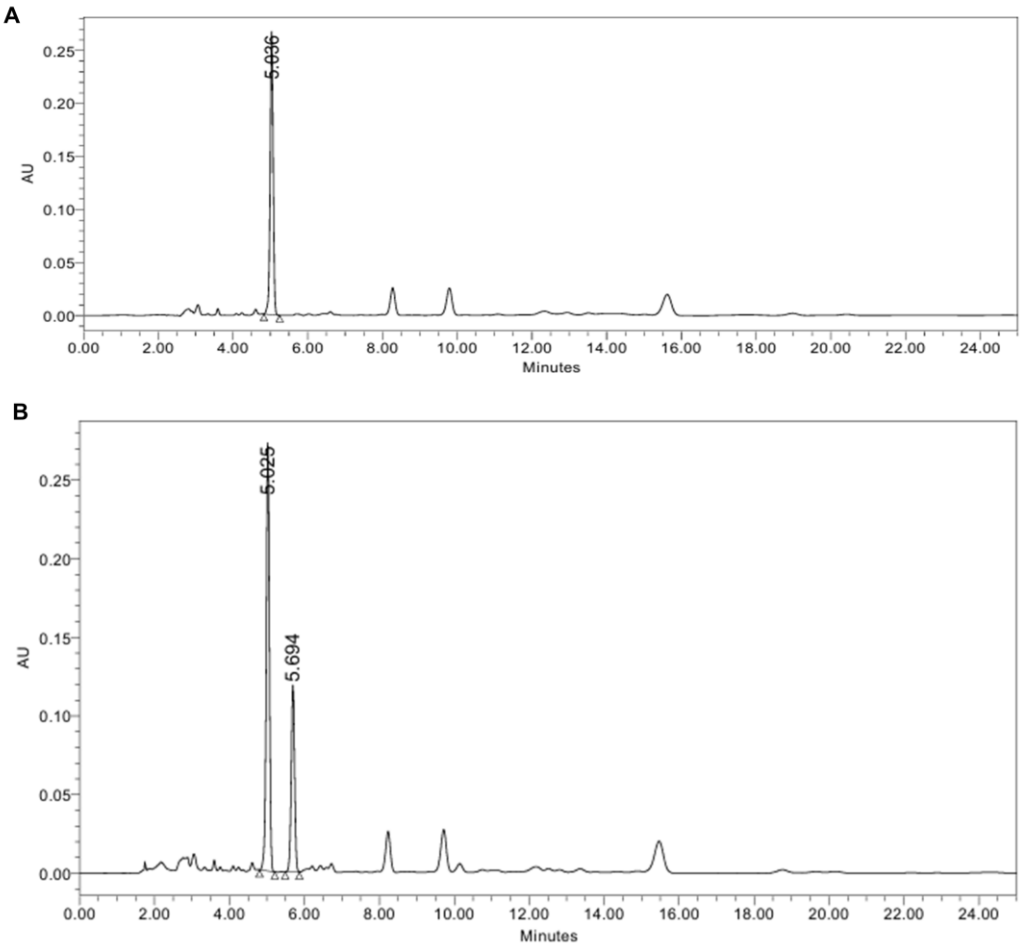

Figure 1. Representative HPLC chromatograms of (A) GE, showing 6-gingerol at 5.036 min, and (B) a GE and LPE mixture, showing a distinct peak for piperine at 5.694 min.

2.2. Animals and Treatments

The animal studies were approved by the Institutional Animal Care and Use Committee of CHA University (approval number: IACUC230174). Five-week-old male ICR mice were purchased from Raon Bio (Yongin, Korea) and housed at 20 ± 3 °C in a room maintained under a 12 h light/12 h dark cycle. After a one-week period of adaptation, the mice were randomly assigned in a blinded manner into four groups (n = 14 per group): a chow diet (Ctrl) group, a high-fat diet (HFD) group, a group

 doi:10.20944/preprints202506.2436.v1

fed HFD supplemented with oral GE at 60 mg/kg/day (GE), or a group fed HFD supplemented with GE and LPE co-administered at 30 mg/kg/day each (GE+LPE). Sample administration was initiated concurrently with HFD feeding to assess both preventive and therapeutic effects of the GE extract and GE+LPE extract. The HFD contained 60 kcal% as fat (D12492, Research Diets, NJ, USA), while the chow diet contained 10 kcal% as fat (D12450B, Research Diets, NJ, USA). Mice were fed both diets for 8 weeks, with weekly measurements of body mass and dietary intake. At the end of the experiment, the mice were euthanized by exposure to carbon dioxide (CO2) until respiratory arrest after fasting for 12 h, then blood and tissue samples were collected.

2.3. Fasting Blood Glucose Measurement

The fasting glucose concentrations were measured weekly from the tail vein after 12 h of fasting using a blood glucose test meter (Accu-Chek, Roche Diagnostics, Basel, Switzerland).

2.4. Oral Glucose Tolerance Test and Insulin Tolerance Test

The oral glucose tolerance test (OGTT) was conducted after a 12-hour fast. D-glucose (1.5 g/kg body weight) was orally administered, and blood glucose concentrations were measured at 0 (baseline), 30, 60, 90, and 120 min after administration using a glucose meter (Accu-Chek, Roche Diagnostics, Basel, Switzerland). Additionally, an Insulin tolerance test (ITT) was performed following the same 12-hour fasting period. Mice received an intraperitoneal injection of insulin (1 U/kg body weight), and blood glucose concentrations were measured at 0 (baseline), 30, 60, 90, 120, and 150 min following the injection.

2.5. Histological Analysis

Samples of subcutaneous (sWAT) and visceral (vWAT) WAT samples were fixed in 4% paraformaldehyde and embedded in paraffin. Several sections were then prepared and stained with hematoxylin and eosin (H&E) for histological assessment. Photomicrographs were obtained using a Nikon E600 microscope (Nikon, Tokyo, Japan).

2.6. Rectal Temperature Measurement

The rectal temperatures of the mice were measured weekly using a Testo 925 Type Thermometer (Testo, Lenzkirch, Germany).

2.7. Immunofluorescence Staining

Samples of sWAT and vWAT sections were deparaffinized and then incubated with anti-PKA or anti-UCP1 antibodies. Subsequently, secondary anti-mouse fluorescein isothiocyanate (FITC)-conjugated and anti-rabbit Alexa Fluor™ 594-conjugated antibodies were then applied. DAPI (Thermo Fisher Scientific, MA, USA) was used to stain the cell nuclei, and the sections were mounted with ProLong Gold Antifade reagent (Thermo Fisher Scientific). Fluorescent images were captured using a Zeiss confocal laser scanning microscope (LSM880; Carl Zeiss, Oberkochen, Germany) along with Zen 3.10 software (Carl Zeiss).

2.8. Biochemical Analysis

Blood samples were obtained through cardiac puncture under terminal anesthesia and centrifuged at 3,000 × g for 20 min at 4°C to separate the serum. The serum concentrations of insulin, leptin, and resistin were measured using a Mouse Adipokine Magnetic Magnetic Bead Panel (Merck Millipore, Burlington, MA, USA). The serum concentrations of the total GLP-1 were measured using a Metabolic Hormone Panel V3 (Merck Millipore, Burlington, MA, USA). Additionally, the serum concentrations of triglycerides (TG), total cholesterol, low-density lipoprotein (LDL)-cholesterol, and high-density lipoprotein (HDL)-cholesterol as well as the activities of aspartate aminotransferase (AST) and alanine aminotransferase (ALT), were measured using colorimetric assay kits from Roche.

 doi:10.20944/preprints202506.2436.v1

2.9. Oil Red O Staining

Cryostat sections of liver tissue (5 μm) were stained with a 0.1% (m/v) Oil Red O (ORO) solution to visualize lipid accumulation in the liver. After staining at room temperature, the sections were rinsed and examined to evaluate the presence and distribution of lipid droplets.

2.10. Western Blot Analysis

Tissues were washed twice with phosphate-buffered saline (PBS) and then lysed using a lysis buffer that included 1 mM phenylmethylsulfonyl fluoride, 1 mM ethylenediaminetetraacetic acid, 1 μM pepstatin A, 1 μM leupeptin, and 0.1 μM aprotinin (iNtRON Biotechnology, Seoul, Korea), along with phosphatase and protease inhibitors. The samples were allowed to stand on ice for 1 hour to facilitate lysis. Following homogenization, the samples were centrifuged at 13,000 × g for 20 min at 4°C. The protein content in the supernatant was determined, and the lysate protein concentrations were quantified using a protein assay kit (Bio-Rad, Hercules, CA, USA). Lysates containing equal amounts of protein were separated using sodium dodecyl sulfate-polyacrylamide gel electrophoresis (SDS-PAGE), and the proteins were electrotransferred to membranes. The membranes were then blocked with 5% skim milk for 1 hour, washed with Tris-buffered saline containing Tween 20 (TBST), and incubated with primary antibodies overnight at 4°C. Subsequently, the membranes were exposed to horseradish peroxidase-conjugated secondary antibodies. Antibodies targeting C/EBPα, PPARγ, FABP4, sterol regulatory element-binding protein 1 (SREBP1), LPAATθ, lipin 1, DGAT1, phosphorylated PKA (p-PKA, Ser 114), α-tubulin, and PGC1α were purchased from Santa Cruz Biotechnology (Dallas, TX, USA). Antibodies targeting ATGL, phosphorylated HSL (p-HSL, Ser 563), Fatty Acid Synthase (FAS) were purchased from Cell Signaling Technology (Danvers, MA, USA). Antibodies targeting MGL, PPARα, PRDM16, and UCP1 were purchased from Abcam (Cambridge, UK).

2.11. Statistical Analysis

Data are expressed as mean ± SEM. Statistical comparisons were made using one-way ANOVA followed by Tukey's post-hoc test (IBM SPSS Statistics Version 20.0, Armonk, NY, USA). $P < 0.05$ was regarded as indicating statistical significance.

3. Results

3.1. GE More Effectively Suppresses HFD-Induced Obesity than GE+LPE

To evaluate the anti-obesity efficacy of GE and its combination with LPE (GE+LPE), mice were fed an HFD for 8 weeks and administered either GE alone or the GE+LPE mixture. At the end of the treatment period, the body mass of mice in the HFD group mice was substantially higher than in the Ctrl group (Figure 2A, B). Both treatment groups showed significantly reduced body mass compared to the HFD group. However, the GE group exhibited a significantly greater reduction in body weight gain compared to the GE+LPE group. This pattern was consistent in both body weight and adipose tissue measurements (Figure 2C, D). The masses of vWAT, sWAT, and perirenal WAT were significantly lower in the GE group compared to the GE+LPE group. In contrast, no significant differences were observed in the masses of organs such as the kidneys, lungs, and spleens across the four groups (Figure 2E). Moreover, no significant differences in food or water intake were observed among the HFD-fed groups (Figure 2F), suggesting that the observed differences in body weight were not due to reduced energy intake.

 doi:10.20944/preprints202506.2436.v1

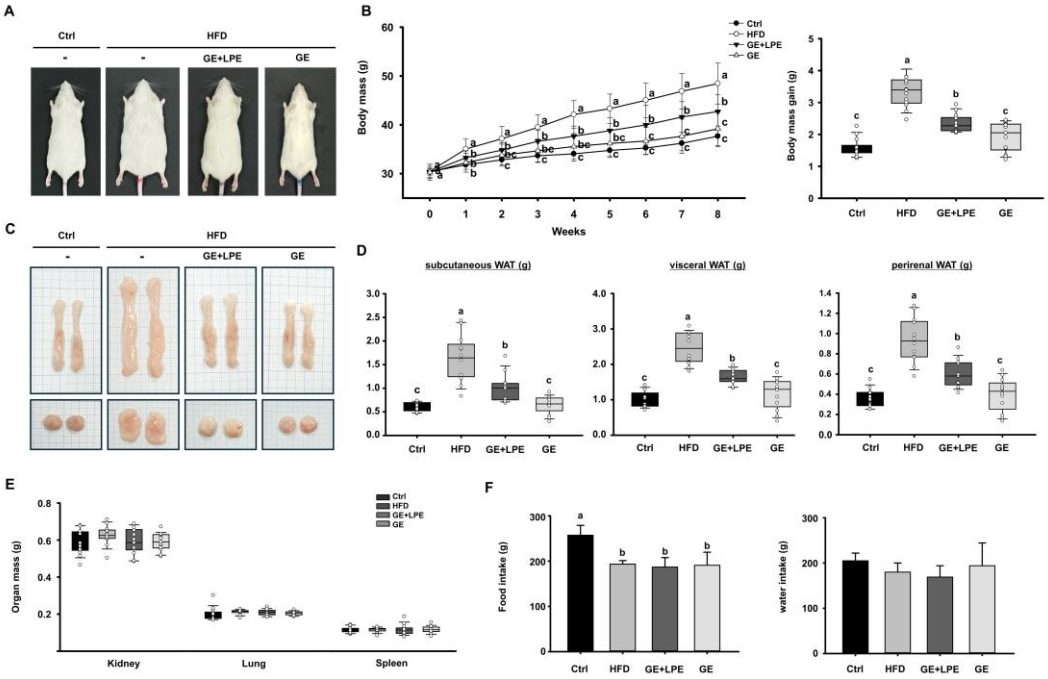

Figure 2. Effects of GE and GE+LPE on body weight, fat mass, and energy intake in HFD-fed mice. (A) Representative images of the mice from each group at the end of the 8-week treatment. (B) Body mass measured regularly during the 8-week treatment and body mass gain over the 8 weeks. (C) Representative images of dissected sWAT (top) and vWAT (bottom). (D) Masses of the sWAT, vWAT, and perirenal WAT. (E) Masses of other organs including kidneys, lungs, and spleen. (F) Food and water intake recorded during the 8-week treatment. Data are expressed as mean ± SEM. Values with different letters are significantly different: $p < 0.05$ (a > b > c).

3.2. GE More Effectively Improves Glucose Homeostasis, and Metabolic Hormone Regulation than GE+LPE

To further evaluate the metabolic effects of GE and GE+LPE, we next assessed glucose intolerance and insulin resistance. Over the 8 weeks of the experiment, the fasting blood glucose concentrations of the HFD group increased gradually, while both treatment groups showed a significant decrease in fasting blood glucose concentrations compared to the HFD group. Notably, the GE group showed a more pronounced reduction than the GE+LPE group (Figure 3A). To assess glucose homeostasis, OGTT and ITT were conducted after the 8 weeks treatment period. As shown in Figure 3B, both the GE and GE+LPE groups displayed significantly lower fasting glucose concentrations and reduced under the curve (AUC) during the OGTT compared to the HFD group, with the GE group demonstrating a more pronounced improvement in glucose regulation. Similarly, the results of the ITT revealed that blood glucose concentrations declined more rapidly in both treatment groups than in the HFD group (Figure 3C). Consistent with these results, serum insulin concentrations were significantly lower in both treatment groups compared to HFD controls, particularly in the GE group (Figure 3D). Additionally, serum concentrations of glucagon-like peptide-1 (GLP-1), an incretin hormone that promotes insulin secretion [32], was significantly elevated in the GE group (Figure 3E).

 doi:10.20944/preprints202506.2436.v1

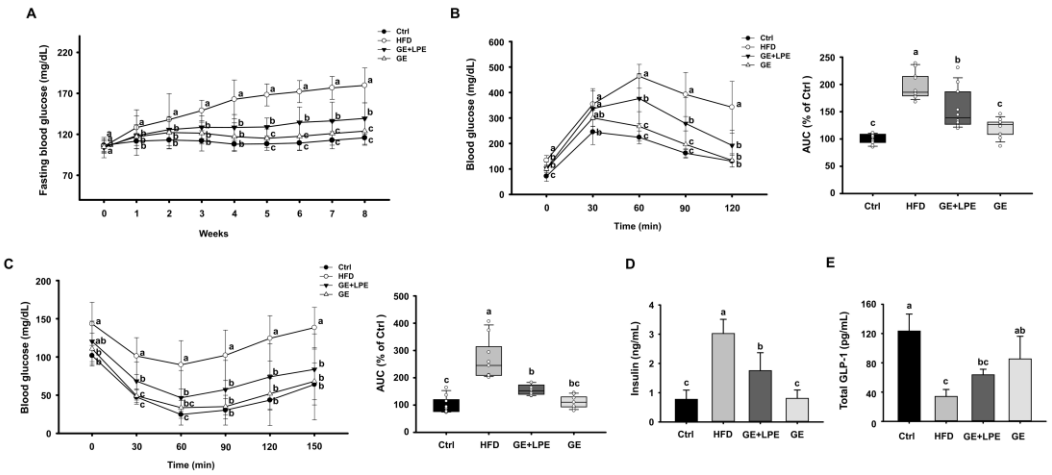

Figure 3. Effects of GE and GE+LPE on the glucose intolerance and insulin resistance of HFD-fed mice. (A) Fasting blood glucose concentrations during the 8-week treatment. (B) Results of oral glucose tolerance test (OGTT) after 8 weeks treatment, and corresponding areas under the curves (AUC). (C) Results of insulin tolerance testing (ITT) after 8 weeks treatment, and corresponding AUC. (D) Serum insulin concentrations, (E) serum GLP-1 concentrations after 8 weeks. Data are expressed as mean ± SEM. Values with different letters are significantly different: $p < 0.05$ (a > b > c).

In addition, GE treatment significantly improved the dysregulated lipid profile induced by HFD, including reductions in triglycerides (TG), total cholesterol, and LDL cholesterol, as well as higher concentrations of HDL-cholesterol (Figure 4A-D). Furthermore, the administration of GE significantly reduced the concentrations of leptin and resistin in serum (Figure 4E, F), which are adipokines closely associated with obesity-related metabolic dysfunction. These findings collectively suggest that GE exerts a more pronounced impact on improving glucose homeostasis, lipid profiles, metabolic hormones compared to GE+LPE in HFD-induced obese mice.

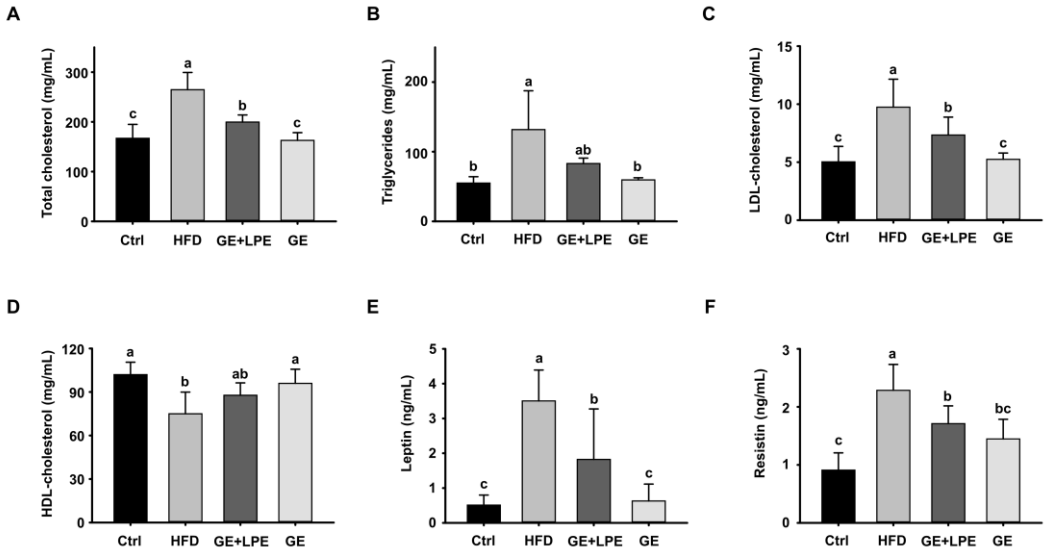

Figure 4. Effects of GE and GE+LPE on lipid profile and adipokine concentrations of HFD-fed mice. (A) Total cholesterol, (B) Triglyceride, (C) LDL-cholesterol, (D) HDL-cholesterol (E) Leptin, and (F) Resistin concentrations after 8-week treatment. Data are expressed as mean ± SEM. Values with different letters are significantly different: $p < 0.05$ (a > b > c).

3.3. GE More Effectively Inhibits Adipogenesis and Lipogenesis in WAT than GE+LPE

H&E staining demonstrated that adipocytes in both sWAT and vWAT of HFD group were markedly larger than those in the Ctrl group (Figure 5A). The quantification confirmed that both GE

 doi:10.20944/preprints202506.2436.v1

and GE+LPE groups significantly reduced adipocyte size and, with a more pronounced effect observed in the GE group (Figure 5B, C). To investigate the underlying mechanisms, the expression of key regulators of adipogenesis (C/EBPα, PPARγ, and FABP4) and lipogenesis (LPAATθ, lipin 1, and DGAT1) was assessed in sWAT and vWAT by western blot analysis. Expression levels of these proteins were significantly increased in the HFD group compared to the Ctrl group. However, the GE group showed a greater suppression of these adipogenic and lipogenic factors than the GE+LPE group (Figure 5D, E). These results indicate that GE more effectively inhibits adipocyte differentiation and lipid accumulation in WAT compared to GE+LPE, thereby contributing to its superior anti-obesity effects in HFD-induced obesity.

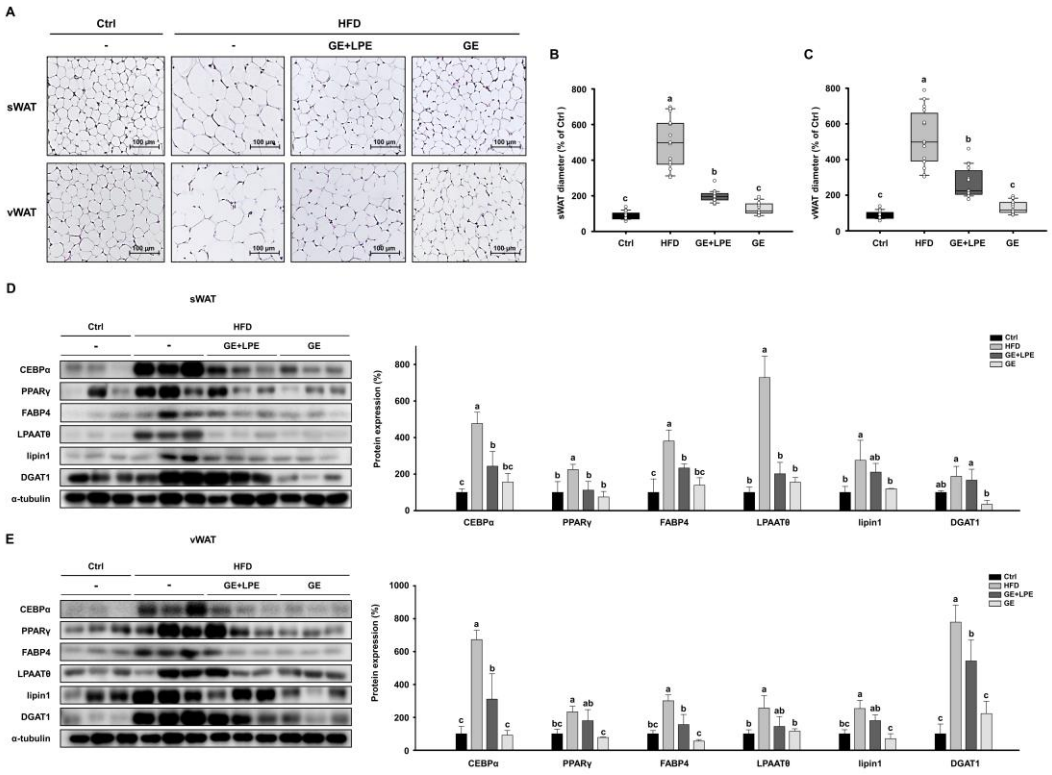

Figure 5. Effects of GE and GE+LPE on adipocyte size and the expression of adipogenic/lipogenic proteins in WAT of HFD-fed mice. (A) Sections of sWAT and vWAT stained with hematoxylin and eosin. Quantification of adipocyte size (B) in the sWAT and (C) in the vWAT. (D) Western blots of adipogenic proteins (C/EBPα, PPARγ, and FABP4) and lipogenic proteins (LPAATθ, lipin1, and DGAT1) in sWAT. (E) Western blots of adipogenic proteins (C/EBPα, PPARγ, and FABP4) and lipogenic proteins (LPAATθ, lipin1, and DGAT1) in vWAT. Protein expression levels were normalized to α-tubulin. Data are expressed as mean ± SEM. Values with different letters are significantly different: $p < 0.05$ (a > b > c).

3.4. GE More Effectively Promotes Lipolysis and Browning in WAT than GE+LPE

To evaluate the thermogenic effects, weekly measurements of rectal temperature were performed. The GE group showed significantly higher rectal temperatures than both the HFD and GE+LPE groups, which may reflect increased thermogenic activity (Figure 6A). Consistent with this finding, immunofluorescence staining showed that the intensity of PKA and UCP1 signals was markedly increased in WAT from GE group compared to the HFD and GE+LPE groups (Figure 6B). To further investigate the molecular mechanisms underlying these effects, we assessed the expression of lipolytic enzymes, including ATGL, p-HSL, and MGL. Both treatment groups exhibited upregulated expressions of these proteins compared to the HFD group, with the GE group displaying a more pronounced increase in lipolytic activity. Additionally, the expression of thermogenic genes such as PPARα, PGC1α, PRDM16, and UCP1 was significantly elevated in both treatment groups, and GE induced a more pronounced upregulation than GE+LPE (Figure 6C, D). Taken together, these

 doi:10.20944/preprints202506.2436.v1

findings suggest that GE promotes WAT browning and thermogenesis more effectively than GE+LPE, likely due to enhanced lipolysis and activation of key thermogenic pathways.

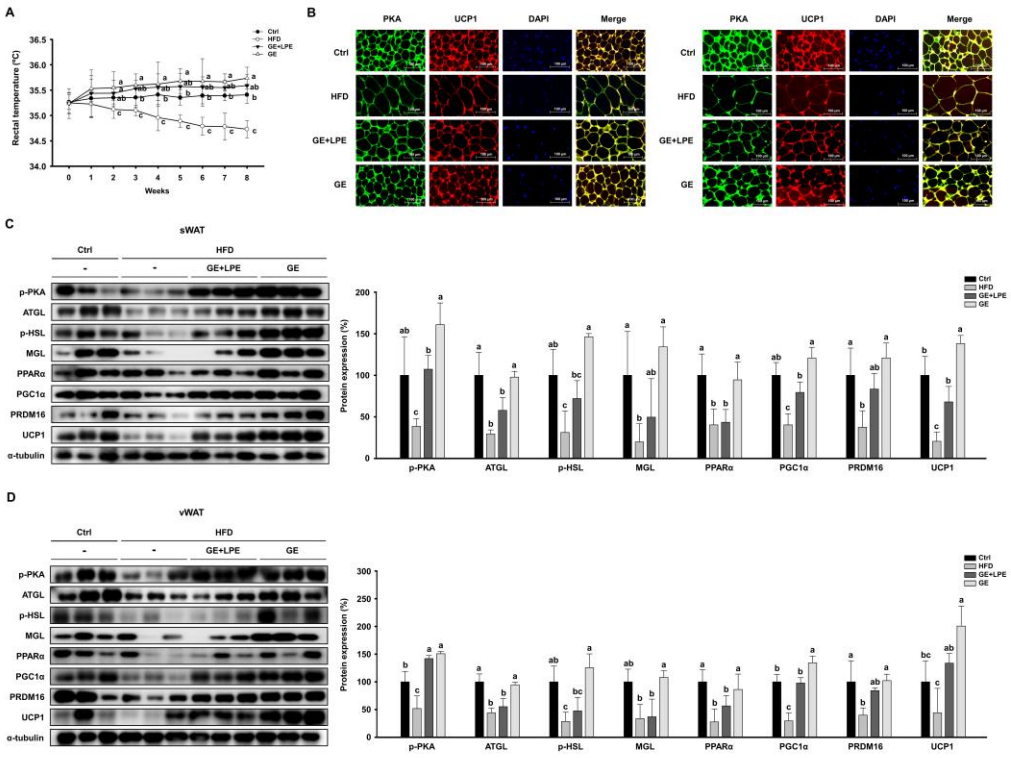

Figure 6. Effects of GE and GE+LPE on lipolysis and browning in the WAT of HFD-fed mice. (A) Rectal temperatures of the mice during 8 weeks of treatment (B) Immunofluorescence staining of PKA and UCP1 in sWAT and vWAT. (C) Western blots of proteins involved in lipolysis (p-PKA, ATGL, p-HSL, and MGL) and browning (PPARα, PGC1α, PRDM16, and UCP1) in sWAT. (D) Western blots of proteins involved in lipolysis (p-PKA, ATGL, p-HSL, and MGL) and browning (PPARα, PGC1α, PRDM16, and UCP1) in vWAT. Protein expression levels were normalized to α-tubulin. Data are expressed as mean ± SEM. Values with different letters are significantly different: $p < 0.05$ (a > b > c).

3.5. GE More Effectively Ameliorates Hepatic Steatosis than GE+LPE

To determine whether GE or GE+LPE could improve obesity-associated hepatic steatosis, we examined liver morphology and lipid accumulation. HFD feeding induced significant hepatic steatosis, as evidenced by pale and enlarged livers. In contrast, livers from the GE group exhibited a darker, healthier appearance comparable to the Ctrl group (Figure 7A). Moreover, serum concentrations of biochemical factors of liver dysfunction, alanine aminotransferase (ALT) and aspartate aminotransferase (AST) were significantly lower in the GE group than in both the HFD and GE+LPE groups (Figure 7B, C). In addition, liver mass was significantly reduced in the GE group compared to both the HFD and GE+LPE groups (Figure 7D). Consistent with these findings, Oil Red O staining showed extensive lipid accumulation in the HFD group, whereas it was more substantially reduced in the GE group than in the GE+LPE group (Figure 7E).

We next examined hepatic expression of key lipogenic proteins including SREBP1, FAS, LPAATθ, lipin1, DGAT1. Although both groups showed reduced expression of lipogenic proteins (Figure 7F), GE induced a greater suppression compared to GE+LPE. This suggests that GE more effectively inhibits hepatic lipid synthesis and steatosis under HFD conditions.

 doi:10.20944/preprints202506.2436.v1

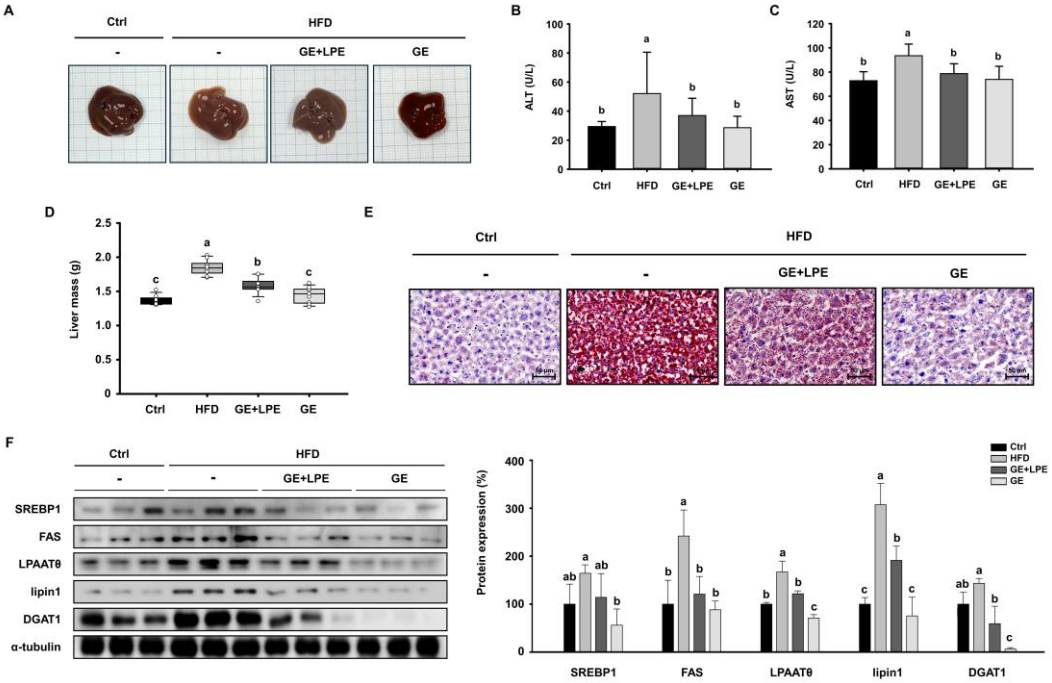

Figure 7. Effects of GE and GE+LPE on hepatic lipid accumulation in HFD-fed mice. (A) Representative images of mouse liver morphology. (B) Serum ALT and (C) AST concentrations. (D) Liver mass. (E) Oil red O-stained liver sections. (F) Western blots of hepatic lipogenic protein expression (SREBP1, FAS, LPAATθ, lipin1, and DGAT1). Protein expression levels were normalized to α-tubulin. Data are expressed as mean ± SEM. Values with different letters are significantly different: $p < 0.05$ (a > b > c).

4. Discussion

The study highlights that GE administration more effectively ameliorates obesity in HFD-fed mice compared to its combination with LPE. While both GE and GE+LPE treatments led to significant reductions in body weight gain, adipose tissue mass, and lipid accumulation, the GE group consistently exhibited superior effects across key metabolic indicators. These findings suggest that the anti-obesity potential of GE may not be synergistically enhanced by co-administration with LPE under the tested dose and ratio.

Improvements in glucose tolerance and insulin sensitivity were observed in both treatment groups with a more pronounced effect in the GE group. The observed effects may primarily result from secondary metabolic improvements resulting from the reduction of excessive adipose tissue. Consistently, OGTT and ITT results demonstrated more rapid and sustained reductions in blood glucose concentrations in the GE group compared to the GE+LPE group, indicating enhanced glucose utilization and insulin sensitivity. This was accompanied by an increase in circulating insulin concentrations. In addition, GLP-1 concentrations were also elevated in the GE group, which may have contributed to the observed improvements in glucose homeostasis by enhancing insulin secretion [33,34]. Moreover, the GE group exhibited improved lipid profiles and reduced circulating concentrations of leptin and resistin, supporting its superior metabolic efficacy compared to GE+LPE [35].

At the tissue level, GE treatment more effectively suppressed both adipogenesis and lipogenesis in WAT. This was reflected not only in the reduction of adipocyte size but also in the decreased expression of transcription factors involved in adipocyte differentiation (C/EBPα, PPARγ, and FABP4) and enzymes regulating lipid synthesis (LPAATθ, lipin 1, and DGAT1). These changes were also accompanied by improvements in hepatic steatosis [36], possibly due to improved lipid metabolism. Alongside these effects, GE enhanced lipolytic activity, as shown by increased levels of ATGL, p-HSL, and MGL. It also promoted thermogenic reprogramming, evidenced by elevated expression of UCP1 and its upstream regulators PPARα, PGC1α, and PRDM16 [37]. Elevated rectal

 doi:10.20944/preprints202506.2436.v1

temperatures and enhanced UCP1 immunoreactivity further substantiated the interpretation that GE promotes energy expenditure through thermogenic activation. These coordinated effects suggest that GE facilitates a functional shift in WAT from lipid storage toward energy dissipation.

In this study, GE (60mg/kg/day) and GE+LPE (1:1 ratio, 30 mg/kg/day each) were orally administered to evaluate their comparative anti-obesity effects in HFD-induced obesity. Despite the well-documented roles of piperine in enhancing bioavailability and modulating lipid metabolism, co-administration of LPE with GE did not confer synergistic benefits in this study. The LPE dose was conservatively determined based on the ADI of piperine established by the EFSA, emphasizing safety but potentially limiting therapeutic efficacy. These findings focus on the superior metabolic efficacy of GE alone and suggesting that under the current conditions, LPE did not enhance the metabolic effects of GE. While alternative dosing regimens or combination proportions may warrant further investigation, the current findings reinforce the robust anti-obesity efficacy of GE alone under HFD conditions. These results highlight the clinical potential of GE as an individual treatment, a naturally derived therapeutic agent for obesity-related metabolic disorders.

5. Conclusions

The present data show that GE alone demonstrated superior anti-obesity effects compared to the GE+LPE mixture in HFD-induced obese mice. These findings support GE as a promising candidate for the prevention and treatment of obesity and related metabolic complications.

Author Contributions: Conceptualization, G.S. and B.Y.L.; methodology, G.S.; software, G.S.; validation, G.S., H.H., H.J and J.K.; formal analysis, G.S.; investigation, G.S.; resources, B.Y.L.; data curation, G.S., H.H.; writing—original draft preparation, G.S.; writing—review and editing, G.S.; visualization, G.S.; supervision, B.Y.L.; project administration, B.Y.L.; funding acquisition, B.Y.L. All authors have read and agreed to the published version of the manuscript.

Funding: This research received no external funding.

Institutional Review Board Statement: All animals were humanely treated according to the standards outlined in the "Guide for the Care and Use of Laboratory Animals" arranged by the National Academy of Science and published by the National Institutes of Health. The study was approved by the Institutional Animal Care and Use Committee of CHA University (Approval Number 230174).

Acknowledgments: We thank Hyeongmin Kim, Yi-Seul Seo, and Heewon Song (Ju Yeong NS Co., Ltd.) for their valuable support in providing experimental materials, technical assistance, and administrative coordination during this study.

References

1. Chandrasekaran, P.; Weiskirchen, R. The role of obesity in type 2 diabetes mellitus—An overview. *International journal of molecular sciences* **2024**, *25*, 1882.
2. Kokkorakis, M.; Chakhtoura, M.; Rhayem, C.; Al Rifai, J.; Ghezzawi, M.; Valenzuela-Vallejo, L.; Mantzoros, C.S. Emerging pharmacotherapies for obesity: a systematic review. *Pharmacological reviews* **2024**, 100002.
3. Saltiel, A.R.; Olefsky, J.M. Inflammatory mechanisms linking obesity and metabolic disease. *The Journal of clinical investigation* **2017**, *127*, 1-4.
4. Rosen, E.D.; Spiegelman, B.M. What we talk about when we talk about fat. *Cell* **2014**, *156*, 20-44.
5. Janochova, K.; Haluzik, M.; Buzga, M. Visceral fat and insulin resistance--what we know? *Biomedical Papers of the Medical Faculty of Palacky University in Olomouc* **2019**, *163*.
6. Radu, F.; Potcovaru, C.-G.; Salmen, T.; Filip, P.V.; Pop, C.; Fierbințeanu-Braticievici, C. The link between NAFLD and metabolic syndrome. *Diagnostics* **2023**, *13*, 614.

 doi:10.20944/preprints202506.2436.v1

7. Godoy-Matos, A.F.; Silva Júnior, W.S.; Valerio, C.M. NAFLD as a continuum: from obesity to metabolic syndrome and diabetes. *Diabetology & metabolic syndrome* **2020**, *12*, 1-20.
8. Scheja, L.; Heeren, J. The endocrine function of adipose tissues in health and cardiometabolic disease. *Nature reviews endocrinology* **2019**, *15*, 507-524.
9. Benomar, Y.; Taouis, M. Molecular mechanisms underlying obesity-induced hypothalamic inflammation and insulin resistance: pivotal role of resistin/TLR4 pathways. *Frontiers in endocrinology* **2019**, *10*, 140.
10. Ghaben, A.L.; Scherer, P.E. Adipogenesis and metabolic health. *Nature reviews Molecular cell biology* **2019**, *20*, 242-258.
11. Liu, F.; He, J.; Wang, H.; Zhu, D.; Bi, Y. Adipose morphology: a critical factor in regulation of human metabolic diseases and adipose tissue dysfunction. *Obesity surgery* **2020**, *30*, 5086-5100.
12. Al-Sayegh, M.; Mahmood, S.; Khair, S.A.; Xie, X.; El Gindi, M.; Kim, T.; Almansoori, A.; Percipalle, P. β-actin contributes to open chromatin for activation of the adipogenic pioneer factor CEBPA during transcriptional reprograming. *Molecular biology of the cell* **2020**, *31*, 2511-2521.
13. Montaigne, D.; Butruille, L.; Staels, B. PPAR control of metabolism and cardiovascular functions. *Nature Reviews Cardiology* **2021**, *18*, 809-823.
14. Prentice, K.J.; Saksi, J.; Hotamisligil, G.S. Adipokine FABP4 integrates energy stores and counterregulatory metabolic responses. *Journal of Lipid Research* **2019**, *60*, 734-740.
15. Lin, S.; Wang, L.; Jia, Y.; Sun, Y.; Qiao, P.; Quan, Y.; Liu, J.; Hu, H.; Yang, B.; Zhou, H. Lipin-1 deficiency deteriorates defect of fatty acid β-oxidation and lipid-related kidney damage in diabetic kidney disease. *Translational Research* **2024**, *266*, 1-15.
16. Yang, W.; Wang, S.; Loor, J.J.; Lopes, M.G.; Zhao, Y.; Ma, X.; Li, M.; Zhang, B.; Xu, C. Role of diacylglycerol O-acyltransferase (DGAT) isoforms in bovine hepatic fatty acid metabolism. *Journal of dairy science* **2022**, *105*, 3588-3600.
17. Coleman, R.A.; Mashek, D.G. Mammalian triacylglycerol metabolism: synthesis, lipolysis, and signaling. *Chemical reviews* **2011**, *111*, 6359-6386.
18. Grabner, G.F.; Xie, H.; Schweiger, M.; Zechner, R. Lipolysis: cellular mechanisms for lipid mobilization from fat stores. *Nature metabolism* **2021**, *3*, 1445-1465.
19. Kloska, A.; Węsierska, M.; Malinowska, M.; Gabig-Cimińska, M.; Jakóbkiewicz-Banecka, J. Lipophagy and lipolysis status in lipid storage and lipid metabolism diseases. *International journal of molecular sciences* **2020**, *21*, 6113.
20. Vagena, E.; Ryu, J.K.; Baeza-Raja, B.; Walsh, N.M.; Syme, C.; Day, J.P.; Houslay, M.D.; Baillie, G.S. A high-fat diet promotes depression-like behavior in mice by suppressing hypothalamic PKA signaling. *Translational psychiatry* **2019**, *9*, 141.
21. Leiria, L.O.; Tseng, Y.-H. Lipidomics of brown and white adipose tissue: Implications for energy metabolism. *Biochimica et Biophysica Acta (BBA)-Molecular and Cell Biology of Lipids* **2020**, *1865*, 158788.
22. Chouchani, E.T.; Kazak, L.; Spiegelman, B.M. New advances in adaptive thermogenesis: UCP1 and beyond. *Cell metabolism* **2019**, *29*, 27-37.
23. Herz, C.T.; Kiefer, F.W. Adipose tissue browning in mice and humans. *Journal of Endocrinology* **2019**, *241*, R97-R109.
24. Ježek, P.; Jabůrek, M.; Porter, R.K. Uncoupling mechanism and redox regulation of mitochondrial uncoupling protein 1 (UCP1). *Biochimica et Biophysica Acta (BBA)-Bioenergetics* **2019**, *1860*, 259-269.
25. Miller, K.N.; Clark, J.P.; Anderson, R.M. Mitochondrial regulator PGC-1a—Modulating the modulator. *Current opinion in endocrine and metabolic research* **2019**, *5*, 37-44.

 doi:10.20944/preprints202506.2436.v1

26. Ebrahimzadeh Attari, V.; Malek Mahdavi, A.; Javadivala, Z.; Mahluji, S.; Zununi Vahed, S.; Ostadrahimi, A. A systematic review of the anti-obesity and weight lowering effect of ginger (Zingiber officinale Roscoe) and its mechanisms of action. *Phytotherapy research* **2018**, *32*, 577-585.
27. Kim, B.; Kim, H.-J.; Cha, Y.-S. The protective effects of steamed ginger on adipogenesis in 3T3-L1 cells and adiposity in diet-induced obese mice. *Nutrition Research and Practice* **2021**, *15*, 279-293.
28. Wang, K.; Kong, L.; Wen, X.; Li, M.; Su, S.; Ni, Y.; Gu, J. The positive effect of 6-Gingerol on High-Fat Diet and Streptozotocin-Induced Prediabetic mice: potential pathways and underlying mechanisms. *Nutrients* **2023**, *15*, 824.
29. Du, Y.; Chen, Y.; Fu, X.; Gu, J.; Sun, Y.; Zhang, Z.; Xu, J.; Qin, L. Effects of piperine on lipid metabolism in high-fat diet induced obese mice. *J. Funct. Foods* **2020**, *71*.
30. Stojanović-Radić, Z.; Pejčić, M.; Dimitrijević, M.; Aleksić, A.; V Anil Kumar, N.; Salehi, B.; C Cho, W.; Sharifi-Rad, J. Piperine-a major principle of black pepper: a review of its bioactivity and studies. *Applied Sciences* **2019**, *9*, 4270.
31. Scientific opinion on flavouring group evaluation 86, revision 2 (FGE.86Rev2): Consideration of aliphatic and arylalkyl amines and amides evaluated by JECFA (65th meeting). **2015**, *13*, 3998, doi:10.2903/j.efsa.2015.3998.
32. Bu, T.; Sun, Z.; Pan, Y.; Deng, X.; Yuan, G. Glucagon-like peptide-1: new regulator in lipid metabolism. *Diabetes & Metabolism Journal* **2024**, *48*, 354-372.
33. Drucker, D.J. GLP-1 physiology informs the pharmacotherapy of obesity. *Molecular Metabolism* **2022**, *57*, 101351.
34. Wharton, S.; Blevins, T.; Connery, L.; Rosenstock, J.; Raha, S.; Liu, R.; Ma, X.; Mather, K.J.; Haupt, A.; Robins, D. Daily oral GLP-1 receptor agonist orforglipron for adults with obesity. *New England Journal of Medicine* **2023**, *389*, 877-888.
35. Giammanco, M.; Marini, H.R.; Pallio, S.; Giammanco, M.M.; Tomasello, G.; Carini, F.; Venturella, F.; Leto, G.; La Guardia, M. Adipokines in obesity and metabolic diseases. *Journal of Biological Research-Bollettino della Società Italiana di Biologia Sperimentale* **2020**, *93*.
36. Seo, S.H.; Fang, F.; Kang, I. Ginger (Zingiber officinale) attenuates obesity and adipose tissue remodeling in high-fat diet-fed C57BL/6 mice. *International Journal of Environmental Research and Public Health* **2021**, *18*, 631.
37. Mishra, B.; Madhu, S.; Aslam, M.; Agarwal, V.; Banerjee, B. Adipose tissue expression of UCP1 and PRDM16 genes and their association with postprandial triglyceride metabolism and glucose intolerance. *Diabetes research and clinical practice* **2021**, *182*, 109115.